

# Optimal Caching in Content-Centric Mobile Hybrid Networks: A Variable Decoupling Approach

Trung-Anh Do, Sang-Woon Jeon, *Member, IEEE*,  
and Won-Yong Shin, *Senior Member, IEEE*

## Abstract

In this paper, large-scale content-centric mobile hybrid networks consisting of mobile nodes and static small base stations (SBSs) (or static helper nodes) are studied, where each node moves according to the random walk mobility model and requests a content object from the library independently at random according to a Zipf popularity distribution. Instead of allowing access to content objects at macro BSs via costly backhaul providing connection to the core network, we consider a more practical and challenging scenario where mobile nodes and SBSs, each having a *finite-size* cache space, are able to cache a subset of content objects so that each request is served by other mobile nodes or SBSs via multihop transmissions. We analyze the optimal throughput–delay trade-off by presenting a new cache allocation strategy using *variable decoupling*. In particular, under a given caching strategy, we first characterize a fundamental throughput–delay trade-off in terms of scaling laws by introducing a general content delivery multihop routing protocol. Then, the optimal throughput–delay trade-off is characterized by presenting the optimal cache allocation strategy, which jointly finds the replication sets at mobile nodes and SBSs via a novel variable decoupling approach. An interesting observation is that highly popular content objects are mainly served by mobile nodes while the rest of content objects are served by static SBSs. We perform numerical evaluation to validate our analytical results. We also show that the optimal strategy strictly outperforms a baseline approach, where the replication sets at mobile nodes and SBSs are optimized separately.

## Index Terms

Caching, content-centric network, mobile hybrid network, throughput–delay trade-off, variable decoupling.

## 1 INTRODUCTION

Mobile data traffic has grown exponentially in recent years [1]. Due to the limitations of subscribers' monthly data plans and limited backhaul links, however, there always exists a gap between the users' expectation and the provided services. For such reasons, a dramatic technological paradigm shift seems to be required in order to support efficient mobile data offloading. To this end, wireless data caching [2], [3] has emerged as a promising technique that deals with the exponential growth of mobile data traffic without introducing costly backhaul (or infrastructure) providing connection to the core network and, therefore, maintaining the sustainability of future wireless networks. The core of wireless data caching is to allow base stations (BSs) or end terminals to cache a subset of content objects. Hence, user requests can be directly served by BSs or end terminals that cached the requested objects, without contacting costly backhaul links.

### 1.1 Prior Work

As the number of users continues to grow dramatically, the capacity scaling law behavior has been widely studied in large-scale wireless networks. In [4], it was shown that for a static ad hoc network consisting of  $n$  randomly distributed

---

- T.-A. Do was with Dankook University, Yongin 16890, Republic of Korea. He is now with the Division of Science and Technology Management and International Cooperation, Posts and Telecommunications Institute of Technology, Hanoi 100000, Vietnam.  
E-mail: anhdt@ptit.edu.vn.
- S.-W. Jeon is with the Department of Military Information Engineering, Hanyang University, Ansan 15588, Republic of Korea.  
E-mail: sangwoonjeon@hanyang.ac.kr.
- W.-Y. Shin is with the Department of Computer Science and Engineering, Dankook University, Yongin 16890, Republic of Korea.  
E-mail: wyshin@dankook.ac.kr

source–destination (S–D) pairs in a unit network area, the per-node throughput of  $\Theta\left(\frac{1}{\sqrt{n \log n}}\right)$  is achievable using the nearest neighbor multihop transmission. There have been further studies on multihop schemes in the literature [5], [6], [7], [8], where the per-node throughput scales far slower than  $\Theta(1)$ . Besides the multihop schemes, there have been various research directions to improve the per-node throughput up to a constant scaling by using hierarchical cooperation [9], node mobility [10], [11], interference alignment [12], directional antennas [13], [14], [15], and infrastructure support [16], [17].

Contrary to the studies on the conventional ad hoc network model in which S–D pairs are given and fixed, investigating *content-centric ad hoc networks* would be quite challenging. As content objects are cached by numerous nodes over a network, finding the closest content holder of each request and scheduling between requests are of crucially importance for improving the overall network performance. The scaling behavior of content-centric ad hoc networks has received a lot of attention in the literature [18], [19], [20], [21], [22], [23]. In *static* ad hoc networks, throughput scaling laws were analyzed using multihop communication [18], [20], which yields a significant performance gain over the single-hop caching scenario in [3], [19]. More specifically, a centralized and deterministic cache allocation strategy was presented in [18], where replicas of each content object are statically determined based on the popularity of each content object in a centralized manner. A decentralized and random cache allocation strategy along with a local multihop protocol was also introduced in [20], where content objects are assigned independently at random to the caches of all users. On the other hand, in *mobile* ad hoc networks, performance on the throughput and delay was examined under a reshuffling mobility model, where the position of each node is independently determined according to random walks with an adjustable flight size and updated at the beginning of each time slot [21]. It was shown in [21] that increasing the mobility degrees of nodes leads to worse performance when deterministic cache allocation is used similarly as in [18]. In addition, caching in ad hoc networks was extended to static infrastructure-supported networks using multihop communication [22], [23]. Specifically, a random caching strategy was used in [22], [23], and each macro BS was assumed to be connected to the core network via infinite-speed backhaul, which has an access to all content objects stored in the whole file library.

Meanwhile, a different caching framework, termed coded caching [24], [25], [26], has received a great deal of attention in cache-enabled wireless networks, where a single transmitter simultaneously deals with several different demands using common coded multicast transmission. Based on this approach, a global caching gain can be achieved by finding the optimal content placement such that multicasting opportunities are exploited simultaneously for all possible requests in the delivery phase.

## 1.2 Main Contributions

In this paper, we study a *large-scale content-centric mobile hybrid network*, where each node moves according to the random walk mobility model (RWMM) and requests a content object from the library independently at random according to a Zipf popularity distribution while multiple small BSs (SBSs) (or helper nodes) are regularly placed over the network area. Instead of assuming an access to the core network through infinite-speed backhaul links that may not work properly during peak hours with heavy traffic, we assume that *each of mobile nodes and SBSs is equipped with a finite-size cache* and is able to cache content objects in the library, which is more feasible in practice. Our caching framework is basically composed of the caching phase and the delivery phase. For a given caching strategy, we first present a content delivery routing protocol with and without SBS support via multihop in order to deliver content objects to requesting nodes, which leads to a fundamental throughput–delay trade-off. Then, we optimize a cache allocation strategy that provides the optimal throughput–delay trade-off. Specifically, unlike all the prior work, we propose a novel *variable decoupling* approach that optimally finds the replication sets for caching at mobile nodes and SBSs, denoted by  $A_m$  and  $B_m$  for content object  $m \in \{1, \dots, M\}$ , respectively, where  $M$  indicates the number of content objects in the library. The proposed approach solves two different convex optimization problems with relaxation based on the relative size of  $A_m$  and  $B_m$ , leading to much simpler analysis compared to tackling the original problem that may not provide a tractable closed-form solution. Our main results reveal that when each SBS has a relatively large-size cache, highly popular content objects are mainly served by mobile nodes whereas the rest of content objects are served by static SBSs. Based on the optimal cache allocation strategy, we finally characterize the optimal throughput–delay trade-off with respect to system parameters.

The main contributions of this paper are summarized as follows:

- We introduce a practical cache-enabled mobile hybrid network configuration where each of mobile nodes and SBSs is equipped with a *finite-size* cache.
- A fundamental throughput–delay trade-off of a content-centric mobile hybrid network in terms of scaling laws is characterized by introducing a content delivery multihop routing protocol with and without SBS support.

- The main challenge resides in establishing the optimal content replication strategy (i.e., the optimal cache allocation strategy), which jointly optimizes the number of replicas cached at mobile nodes and SBSs, denoted by  $A_m$  and  $B_m$  for  $m \in \{1, \dots, M\}$ , respectively, via nontrivial variable decoupling. An interesting observation is that when the total cache space at all SBSs is greater than that at all mobile nodes, highly popular contents are stored mainly in node caches while any request for less popular contents is fulfilled by SBSs.
- We then analyze the optimal throughput–delay trade-off according to the identified operating regimes with respect to four scaling parameters.
- We validate our analysis by numerically showing our optimal solution to the cache allocation problem, which exhibits that the numerical results are consistent with the analytical trend.
- For comparison, we also present a baseline strategy that optimizes the replication sets at nodes and SBSs in a *separate* manner and show that it is strictly suboptimal.

### 1.3 Organization

The rest of this paper is organized as follows. In Section II, the network model and performance metrics under consideration are described. In Section III, the content delivery routing protocol is presented. In Section IV, a fundamental throughput–delay trade-off is introduced in terms of scaling laws. In Section V, the optimal throughput–delay trade-off is derived by introducing the optimal cache allocation strategy using variable decoupling. A baseline strategy is also shown in Section VI for comparison. Finally, Section VII summarizes the paper with some concluding remarks.

### 1.4 Notations

Throughout this paper,  $\mathbb{E}[\cdot]$  and  $\Pr(\cdot)$  are the expectation and the probability, respectively. Unless otherwise stated, all logarithms are assumed to be to the base 2. We also use the following asymptotic notation: i)  $f(x) = O(g(x))$  means that there exist constants  $C$  and  $c$  such that  $f(x) \leq Cg(x)$  for all  $x > c$ ; ii)  $f(x) = o(g(x))$  means that  $\lim_{x \rightarrow \infty} \frac{f(x)}{g(x)} = 0$ ; iii)  $f(x) = \Omega(g(x))$  if  $g(x) = O(f(x))$ ; iv)  $f(x) = \omega(g(x))$  if  $g(x) = o(f(x))$ ; and v)  $f(x) = \Theta(g(x))$  if  $f(x) = O(g(x))$  and  $f(x) = \Omega(g(x))$  [27].

## 2 NETWORK MODEL AND PERFORMANCE METRICS

In this section, we first describe the network model and then define performance metrics used in the paper.

### 2.1 Network Model

We consider a content-centric mobile hybrid network consisting of  $n$  mobile nodes and  $f(n) = \Theta(n^\delta)$  static SBSs (or static helper nodes), where  $0 \leq \delta < 1$ . We assume that  $n$  nodes are distributed uniformly at random over a unit square and  $f(n)$  SBSs are regularly placed over the same area. That is, the network is divided into  $f(n)$  square SBS cells of equal size given by  $b(n)$  so that each cell has one SBS at its center. The mobility trace of nodes is modelled according to the RWMM [11]. In particular, the unit area is divided into  $n$  square subcells of area  $\frac{1}{n}$ . Each node independently performs a simple random walk with a distance  $\frac{1}{\sqrt{n}}$  on the  $\sqrt{n} \times \sqrt{n}$  disjoint subcells so that the node is equally likely to be in any of the four adjacent subcells after each time slot.

In our content-centric mobile hybrid network, each node and SBS are assumed to be equipped with local caches, which are installed to store a subset of content objects in the library of size  $M = \Theta(n^\gamma)$ , where  $0 < \gamma < 1$ . Every content object is assumed to have the same size. In this paper, we consider a more practical cache-enabled network model by assuming that each node and SBS are able to cache at most  $K_n = \Theta(1)$  and  $K_{SBS} = \Theta(n^\beta)$  content objects in their own finite-size caches, respectively, where  $0 < \beta < \gamma$ . We focus on the case that the total cache size in SBSs scales no slower than the total cache size of mobile nodes in the network, i.e.,  $\delta + \beta \geq 1$ , in order to analyze the impact and benefits of SBSs equipped with a relatively large-size cache.<sup>1</sup>

We assume that every node requests its content object independently according to a Zipf popularity distribution, which typically characterizes a popularity of various kinds of real data such as web, file sharing, user-generated content, and video on demand [28]. That is, the request probability of content object  $m \in \mathcal{M} \triangleq \{1, \dots, M\}$  is given by<sup>2</sup>

$$p_m = \frac{m^{-\alpha}}{H_\alpha(M)}, \quad (1)$$

1. Otherwise, the use of SBSs would not be beneficial in improving performance on the throughput and delay in our network model.  
2. Without loss of generality, we assume a descending order between the request probabilities of the  $M$  content objects in the library.

where  $\alpha > 0$  is the Zipf exponent and  $H_\alpha(M) = \sum_{i=1}^M i^{-\alpha}$  is a normalization constant formed in the Riemann zeta function and is given by

$$H_\alpha(M) = \begin{cases} \Theta(1) & \text{for } \alpha > 1 \\ \Theta(\log M) & \text{for } \alpha = 1 \\ \Theta(M^{1-\alpha}) & \text{for } \alpha < 1. \end{cases} \quad (2)$$

In content-centric networks, a caching problem is generally partitioned into the caching phase and the delivery phase. That is, the problem consists of storing content objects in the caches and establishing efficient delivery routing paths for the requested content objects.

We first consider the caching phase, which selects the content objects to be stored in the caches of  $n$  nodes and  $f(n)$  SBSs. Let  $A_m$  and  $B_m$  denote the number of replicas of content object  $m \in \mathcal{M}$  stored at nodes and SBSs, respectively, which will be optimized later. In order for a cache allocation to be feasible,  $\{A_m\}_{m=1}^M$  and  $\{B_m\}_{m=1}^M$  should satisfy the following total caching constraints:

$$\begin{cases} \sum_{m=1}^M A_m \leq nK_n, \\ \sum_{m=1}^M B_m \leq f(n)K_{SBS}. \end{cases} \quad (3)$$

Furthermore, we impose the following individual caching constraints:

$$\begin{cases} A_m \leq n, \\ B_m \leq f(n), \\ A_m + B_m \geq 1 \end{cases} \quad (4)$$

for all  $m \in \mathcal{M}$ . Note that the last constraint in (4) is needed to avoid an outage event such that a requested content object is not stored in the entire network. Similarly as in [18], [21], we employ the *random caching* strategy such that the sets of replicas satisfying (3) and (4) are stored uniformly at random over the caches in  $n$  nodes and  $f(n)$  SBSs.

Now, let us consider the delivery phase of the requested content objects, which allows the requested content objects to be delivered to the corresponding nodes over wireless channels. During the delivery phase, each node downloads its requested content object (possibly via multihop) from one of the nodes or SBSs storing the requested content object in their caches. We adopt the *protocol model* [4] for successful content delivery. In particular, let  $d(u, v)$  denote the Euclidean distance between nodes  $u$  and  $v$ . Then, content delivery from node  $u$  to node  $v$  is assumed to be successful if and only if  $d(u, v) \leq r$  and there is no other active transmitter in a circle of radius  $(1 + \Delta)r$  from node  $v$ , where  $r$  and  $\Delta > 0$  are given protocol parameters.

For analytical tractability, we also adopt the fluid model in [11]. In this model, the size of each content object is assumed to be arbitrarily small. Accordingly, the time required for content delivery between a node and its neighbor node or an assigned SBS is much smaller than the duration of each time slot. Thus, all content objects waiting for transmission at a node will be transmitted by the node within one time slot. However, a content object received by a node at a given time slot cannot be transmitted by the node until the next time slot.

## 2.2 Performance Metrics

Since every content object is assumed to have the same size, we consider the per-node throughput  $\lambda(n)$ , i.e., the rate at which the request of any node in the network can be served according to a given feasible content delivery routing. We make slight modifications to the definitions of throughput and delay in [11] to fit into our content-centric mobile hybrid network, which are provided as follows.

**Definition 1** (Throughput). *Let  $B(i, t)$  denote the total number of bits of the requested content objects received by node  $i$  during  $t$  time slots. Note that this could be a random quantity for a given network realization. Then, the per-node throughput  $\lambda(n)$  is said to be achievable if there exists a sequence of events  $A(n)$  such that*

$$A(n) = \left\{ \min_{1 \leq i \leq n} \liminf_{t \rightarrow \infty} \frac{1}{t} B(i, t) \geq \lambda(n) \right\}$$

and  $\Pr(A(n))$  approaches one as  $n$  tends to infinity.

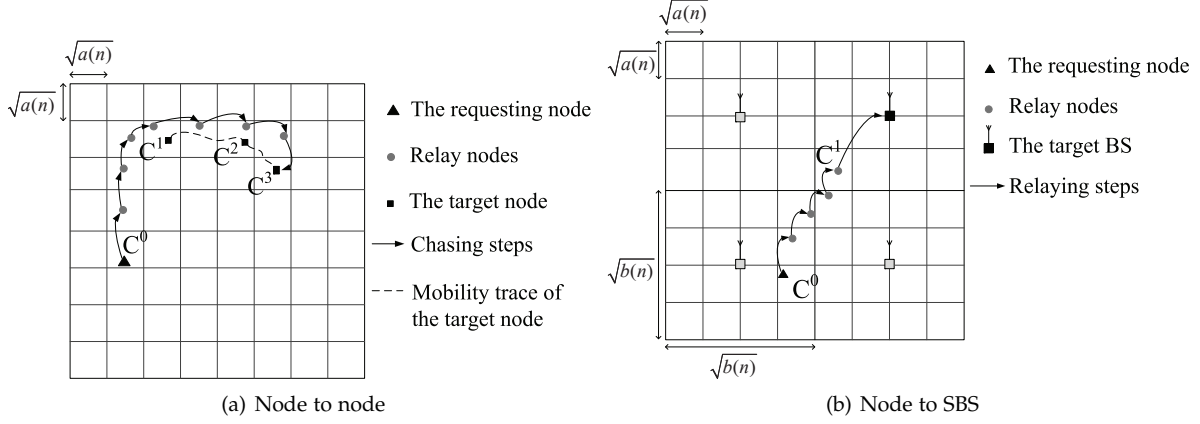


Fig. 1. The first phase of the content delivery routing.

**Definition 2 (Delay).** Let  $D(i, k)$  denote the delay of the  $k$ th requested content object of node  $i$ , which is measured from the moment that the requesting message leaves node  $i$  until the corresponding content object arrives at the node from the closest holder. For a particular realization of the network, the delay for node  $i$  is  $\limsup_{r \rightarrow \infty} \frac{1}{r} \sum_{k=1}^r D(i, k)$ . Then, the delay is defined as the expectation of the average delay of all nodes over all network realizations, i.e.,

$$D(n) \triangleq \mathbb{E} \left[ \frac{1}{n} \sum_{i=1}^n \limsup_{r \rightarrow \infty} \frac{1}{r} \sum_{k=1}^r D(i, k) \right].$$

### 3 CONTENT DELIVERY ROUTING PROTOCOL IN MOBILE HYBRID NETWORKS

In this section, we describe our routing protocol to deliver content objects to requesting nodes. Due to the node mobility, our routing protocol is basically built upon the nearest neighbor multihop routing scheme in [11] and reconstructed for our cache-enabled setting accordingly. For multihop transmission, the network of unit area is divided into  $a(n)^{-1}$  square routing cells of equal size, where  $a(n) = \Omega\left(\frac{\log n}{n}\right)$  and  $a(n) = O(1)$ , so that each routing cell has at least one node with high probability (whp) (see [4] for the details). We implement a multihop routing strategy for content delivery based on routing cells and SBS cells whose size is  $a(n)$  and  $b(n)$ , respectively. Each routing cell is activated regularly once every  $1+c$  time slots to avoid any collision, where  $c > 0$  denotes a small integer independent of  $n$ . Similarly, each SBS cell is activated regularly once every  $1+c$  time slots.

Our content delivery routing protocol operates depending on the network topology, i.e., the initial geographic distance between a requesting node and its closest holder. The requesting node first finds its closest holder (in the Euclidean distance) of the desired content object among  $A_m$  nodes and  $B_m$  SBSs. Then, a requesting message is delivered to the closest holder along the adjacent routing cells via multihop in forward direction, which corresponds to the first phase of the content delivery. Similarly, the desired content object chases the requesting node moving according to the RWMM via multihop in backward direction, which corresponds to the second phase. Each time slot is divided into two sub-slots. The first and second phases of the content delivery procedure are activated during the first and the second sub-slots, respectively. For the case where the requesting node is inside the transmission range of any holder of the desired content object, the request will be served using single-hop transmission within one time slot.

The detailed content delivery procedure is described as follows:

#### Step 1) First delivery phase

- If the closest holder is a mobile node, then the requesting message chases the target node according to the following procedure. As depicted in Fig. 1(a), from routing cell  $C^0$ , the requesting message is transmitted via multihop along the adjacent routing cells toward routing cell  $C^1$  containing the target node, where the per-hop distance is given by  $\Theta(\sqrt{a(n)})$ . By the time the requesting message reaches routing cell  $C^1$ , the target node has moved to another position  $C^2$  with the mobility trace based on the RWMM. Thus, the message hops from routing cell  $C^1$  to routing cell  $C^2$ . This continues until the message reaches the routing cell  $C^3$  containing its target node.
- As depicted in Fig. 1(b), if the closest holder is a SBS, then the requesting message is delivered via multihop along the adjacent routing cells intersecting the straight line toward the coverage of the target SBS, where the per-hop distance

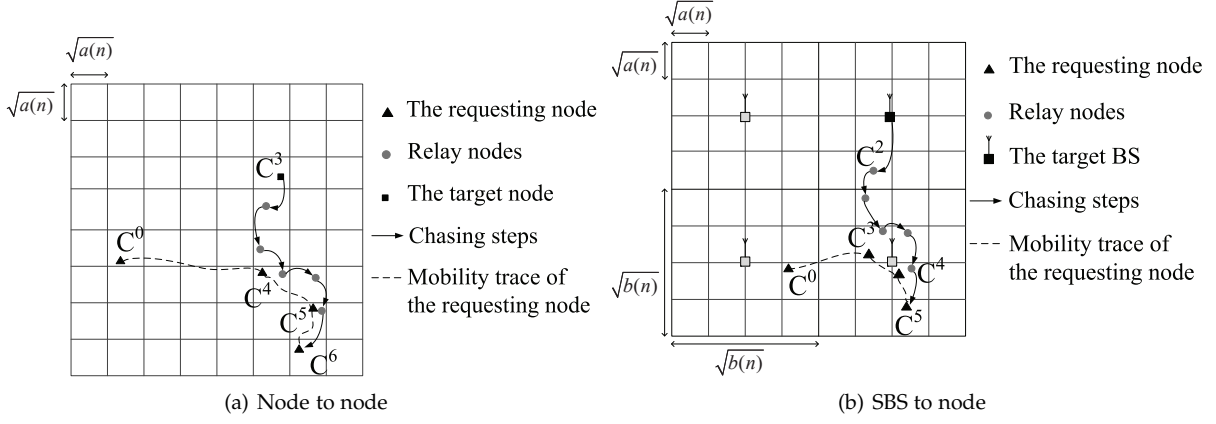


Fig. 2. The second phase of the content delivery routing.

is given by  $\Theta(\sqrt{a(n)})$ . When the requesting message arrives at a node in routing cell  $C^1$  that is inside the SBS cell coverage of the target SBS, the last relay node will send the message to the SBS immediately using single-hop within one time slot, where the last hop distance to the target SBS is given by  $\Theta(\sqrt{b(n)})$ . This long-distance hop for the last hop to the SBS leads to the best performance (which will be specified later).

#### Step 2) Second delivery phase

- By the time the target node receives the requesting message, the requesting node has moved to another position  $C^4$  with the mobility trace based on the RWMM. As illustrated in Fig. 2(a), the desired content object delivered by the target node chases the requesting node by executing essentially the same procedure as the first delivery phase.
- By the time the SBS receives the requesting message, the requesting node has moved to another position  $C^3$ . As illustrated in Fig. 2(b), the desired content object delivered by the SBS is delivered to a relay node in routing cell  $C^2$  along another straight line toward the requesting node within one time slot. Thereafter, the relay chases the requesting node via multihop until reaching the routing cell containing the requesting node.

## 4 THROUGHPUT-DELAY TRADE-OFF

In this section, we characterize a fundamental throughput-delay trade-off in terms of scaling laws for the content-centric mobile hybrid network using the proposed content delivery routing. As stated in Section 3, we consider the nearest neighbor multihop transmission between a requesting node and its closest holder of the desired content object, where their distance is crucially determined by the total number of replicas of content object  $m \in \mathcal{M}$ ,  $A_m + B_m$ . When replicas of each content object are independently and uniformly distributed in the caching phase, the average Euclidean distance from a requesting node to its closest holder was shown to scale as the reciprocal of the square root of the total number of holders of the desired content object in the network [22], [23]. By applying this argument to our mobile hybrid network framework, we establish the following lemma, which is essential to characterize the throughput-delay trade-off.

**Lemma 1.** *For any mobile node requesting content object  $m \in \mathcal{M}$ , the average initial distance between any requesting node and its closest holder of content object  $m$  is  $\Theta(\frac{1}{\sqrt{A_m + B_m}})$ , where  $A_m$  and  $B_m$  are the number of replicas of content object  $m$  stored at nodes and SBSs, respectively.*

*Proof:* The detailed proof of this argument is omitted here since it basically follows the same line as the proof of [22, Lemma 3].  $\square$

We are now ready to show our first main result.

**Theorem 1.** *Suppose that the content delivery routing in Section 3 is used for the content-centric mobile hybrid network. Then, the throughput-delay trade-off is given by*

$$\lambda(n) = \Theta\left(\frac{D(n)}{n \left(\sum_{m=1}^M \frac{p_m}{\sqrt{A_m + B_m}}\right)^2}\right) \quad (5)$$

whp, where

$$\lambda(n) = O\left(\frac{1}{\sum_{m=1}^M p_m \sqrt{\frac{n \log n}{A_m + B_m}}}\right)$$

and  $p_m$  is the request probability of content object  $m \in \mathcal{M}$ .

*Proof.* We apply the approach in [11] to compute the initial distance of a randomly selected S-D pair into our cache-enabled network setting. Then, the length of the routing path of a requesting message or a desired content object is shown to be determined by the initial distance between a requesting node and its closest holder of the desired content object, which is given by  $\Theta\left(\frac{1}{\sqrt{A_m + B_m}}\right)$  from Lemma 1. As a result, the total number of hops along the routing paths of both the requesting message and desired content object scales as  $\Theta\left(\frac{1}{\sqrt{a(n)(A_m + B_m)}}\right)$ . Since in our network, the average delay  $D(n)$  is determined by the time taken from the moment that the requesting message leaves until the desired content object arrives at the requesting node, we have

$$D(n) = \Theta\left(\sum_{m=1}^M \frac{p_m}{\sqrt{a(n)(A_m + B_m)}}\right), \quad (6)$$

where  $p_m$  is the probability that each node requests content object  $m \in \mathcal{M}$ .

Similarly as in [11], from the fact that the number of content objects passing through an arbitrary routing cell in each time slot is given by  $O\left(n \sum_{m=1}^M p_m \sqrt{\frac{a(n)}{A_m + B_m}}\right)$  whp, the average per-node throughput is given by

$$\lambda(n) = \Theta\left(\frac{1}{n \sum_{m=1}^M p_m \sqrt{\frac{a(n)}{A_m + B_m}}}\right) \text{whp}, \quad (7)$$

which is maximized when  $a(n) = \Theta\left(\frac{\log n}{n}\right)$ . Hence, using (6) and (7) leads to (5), which completes the proof of the theorem.  $\square$

Theorem 1 implies that the throughput-delay trade-off is influenced by the total number of replicas of each content object  $m$ , i.e.,  $A_m + B_m$ . Due to the caching constraints in (3) and (4), it is not straightforward how to optimally allocate the sets of replicas,  $\{A_m\}_{m=1}^M$  and  $\{B_m\}_{m=1}^M$ , to show a net improvement in the overall throughput-delay trade-off. In the next section, we introduce the optimal cache allocation strategy to characterize the optimal throughput-delay trade-off.

**Remark 1.** *Based on the above result, it is not difficult to show that if content delivery is performed via multihop, then the throughput-delay trade-off for mobile ad hoc networks is identical to that for static ad hoc networks in [22], [23]. That is, we may conclude that performance on throughput-delay trade-off of both cache-enabled networks is the same as far as the content delivery multihop routing protocols are employed.*

According to the same analysis in [23], the optimal throughput-delay trade-off in Theorem 1 is thus given by  $\lambda(n) = \Theta(D(n))$  when  $\alpha \geq 3/2$ , which is achievable by using node-to-node multihop communication without SBS support. Therefore, for the rest of this paper, we focus on the case where  $\alpha < 3/2$  in solving the optimal content replication problem.

## 5 OPTIMAL CACHE ALLOCATION STRATEGY IN MOBILE HYBRID NETWORKS

In this section, we characterize the optimal throughput-delay trade-off of the content-centric mobile hybrid network by optimally selecting the replication sets  $\{A_m\}_{m=1}^M$  and  $\{B_m\}_{m=1}^M$ . We first introduce our problem formulation in terms of maximizing the throughput-delay trade-off. Then, we propose a content replication strategy that jointly finds the number of replicas cached at mobile nodes and SBSs, thus leading to the optimal throughput-delay trade-off of our content-centric mobile hybrid network. Finally, We validate our analysis by numerically showing our optimal solution to the cache allocation problem.

### 5.1 Problem Formulation

From Theorem 1, it is shown that maximizing the throughput-delay trade-off is equivalent to minimizing the term  $\sum_{m=1}^M \frac{p_m}{\sqrt{A_m + B_m}}$  in (5). From the caching constraints in (3) and (4), we formulate the following optimization problem:

$$\min_{\{A_m\}_{m=1}^M, \{B_m\}_{m=1}^M} \sum_{m=1}^M \frac{p_m}{\sqrt{A_m + B_m}} \quad (8a)$$

$$\text{subject to } \sum_{m=1}^M A_m \leq nK_n, \quad (8b)$$

$$\sum_{m=1}^M B_m \leq f(n)K_{SBS}, \quad (8c)$$

$$A_m \leq n \text{ for } m \in \mathcal{M}, \quad (8d)$$

$$B_m \leq f(n) \text{ for } m \in \mathcal{M}, \quad (8e)$$

$$A_m + B_m \geq 1 \text{ for } m \in \mathcal{M}. \quad (8f)$$

From the fact that the second derivatives of the objective function (8a) with respect to  $A_m$  and  $B_m$  for  $\forall m \in \mathcal{M}$  are non-negative, it is straightforward to preserve the convexity of the objective function [29]. Note that the numbers of replicas of content object  $m$  stored at nodes and SBSs, corresponding to  $A_m$  and  $B_m$ , respectively, are integer variables, which makes the optimization problem non-convex and thus intractable. However, as long as scaling laws are concerned in this work, the discrete variables  $A_m$  and  $B_m$  for  $m \in \mathcal{M}$  can be relaxed to real numbers in  $[1, \infty)$  so that the objective function in (8a) becomes convex and differentiable. In addition, since all inequality constraints (8b)–(8f) are linear functions, the problem in (8) can be a convex optimization problem.

## 5.2 Analytical Results

Since the objective function is convex, we are able to use the Lagrangian relaxation method for solving the problem in (8). In our work, we apply a novel *variable decoupling* technique for the replication sets  $\{A_m\}_{m=1}^M$  and  $\{B_m\}_{m=1}^M$ , which leads to a much simpler analysis without fundamentally changing the original problem in (8) in terms of scaling laws, compared to tackling the original problem that may not provide a tractable closed-form solution. Notice that the total number of replicas of content object  $m \in \mathcal{M}$ ,  $A_m + B_m$ , can be simplified as  $\Theta(A_m)$  or  $\Theta(B_m)$  according to the relative size of  $A_m$  and  $B_m$ . For analytical convenience, given the optimal solution  $\{A_m^*\}_{m=1}^M$  and  $\{B_m^*\}_{m=1}^M$ , let us define two subsets  $\mathcal{M}_1$  and  $\mathcal{M}_2$  as the sets of content objects such that  $A_m^* + B_m^* = \Theta(A_m^*)$  and  $A_m^* + B_m^* = \Omega(f(n))$ , respectively, which will be specified in Theorem 2. We also define the subset  $\mathcal{M}_3$  as the set of content objects such that  $A_m^* + B_m^* = \Theta(B_m^*)$ . Note that for  $m \in \mathcal{M}_3$ ,  $A_m = O(B_m) = O(f(n))$ . Then, the optimization problem in (8) is divided into the following two optimization problems:

$$\min_{\{A_m\}_{m \in \mathcal{M}_1}} \sum_{m \in \mathcal{M}_1} \frac{p_m}{\sqrt{A_m}} \quad (9a)$$

$$\text{subject to } \sum_{m=1}^M A_m \leq nK_n, \quad (9b)$$

$$A_m \leq n \text{ for } m \in \mathcal{M}_1 \quad (9c)$$

and

$$\min_{\{B_m\}_{m \in \mathcal{M}_3}} \sum_{m \in \mathcal{M}_3} \frac{p_m}{\sqrt{B_m}} \quad (10a)$$

$$\text{subject to } \sum_{m=1}^M B_m \leq f(n)K_{SBS}, \quad (10b)$$

$$B_m \leq f(n) \text{ for } m \in \mathcal{M}_3. \quad (10c)$$

The Lagrangian function corresponding to (9) is given by

$$\begin{aligned} \mathcal{L}_1 & (\{A_m\}_{m \in \mathcal{M}_1}, \lambda, \{w_m\}_{m \in \mathcal{M}_1}) \\ &= \sum_{m \in \mathcal{M}_1} \frac{p_m}{\sqrt{A_m}} + \lambda \left( \sum_{m=1}^M A_m - nK_n \right) + \sum_{m \in \mathcal{M}_1} w_m (A_m - n), \end{aligned} \quad (11)$$

where  $w_m, \lambda \in \mathbb{R}$ . The Karush–Kuhn–Tucker (KKT) conditions for (9) are then given by

$$\frac{\partial \mathcal{L}_1(\{A_m^*\}_{m \in \mathcal{M}_1}, \lambda^*, \{w_m^*\}_{m \in \mathcal{M}_1})}{\partial A_m^*} = 0 \quad (12)$$

$$\lambda^* \geq 0$$

$$w_m^* \geq 0$$

$$w_m^*(A_m^* - n) = 0 \quad (13)$$

$$\lambda^* \left( \sum_{m=1}^M A_m^* - nK_n \right) = 0 \quad (14)$$

for  $m \in \mathcal{M}_1$ . Similarly, the Lagrangian function corresponding to (10) is

$$\begin{aligned} \mathcal{L}_2(\{B_m\}_{m \in \mathcal{M}_3}, \mu, \{\nu_m\}_{m \in \mathcal{M}_3}) \\ = \sum_{m \in \mathcal{M}_3} \frac{p_m}{\sqrt{B_m}} + \mu \left( \sum_{m=1}^M B_m - f(n)K_{SBS} \right) + \sum_{m \in \mathcal{M}_3} \nu_m (B_m - f(n)), \end{aligned} \quad (15)$$

where  $\nu_m, \mu \in \mathbb{R}$ . Then for  $\forall m \in \mathcal{M}_3$ , the KKT conditions for (10) state that

$$\begin{aligned} \frac{\partial \mathcal{L}_2(\{B_m^*\}_{m \in \mathcal{M}_3}, \mu^*, \{\nu_m^*\}_{m \in \mathcal{M}_3})}{\partial B_m^*} = 0 \\ \mu^* \geq 0 \\ \nu_m^* \geq 0 \\ \nu_m^*(B_m^* - f(n)) = 0 \\ \mu^* \left( \sum_{m=1}^M B_m^* - f(n)K_{SBS} \right) = 0. \end{aligned} \quad (16)$$

We start from introducing the following lemma, which plays an important role in solving our content replication problem.

**Lemma 2.** Suppose that  $\alpha < 3/2$  and the content delivery routing in Section 3 is used for the content-centric mobile hybrid network. Then, the optimal solution to (9), denoted by  $A_m^*$ , is non-increasing with  $m \in \mathcal{M}_1$  and the optimal solution to (10), denoted by  $B_m^*$ , is non-increasing with  $m \in \mathcal{M}_3$ .

*Proof:* Refer to Appendix A. □

From the above lemma, the following important theorem can be established, which shows the optimal total number of replicas of contents  $m \in \mathcal{M}$  at both nodes and SBSs.

**Theorem 2.** Suppose that  $\alpha < 3/2$  and the content delivery routing in Section 3 is used for the content-centric mobile hybrid network. If  $\alpha \leq \frac{3(\gamma-\beta)}{2(\delta+\gamma-1)}$ , then the optimal solution to (8) is given by

$$A_m^* + B_m^* = \Theta \left( m^{-\frac{2\alpha}{3}} n^{\beta+\delta-\gamma(1-\frac{2\alpha}{3})} \right).$$

If  $\frac{3(\gamma-\beta)}{2(\delta+\gamma-1)} < \alpha < \frac{3}{2}$ , then it is given by

$$A_m^* + B_m^* = \begin{cases} \Theta \left( m^{-\frac{2\alpha}{3}} n^{\delta+(1-\delta)\frac{2\alpha}{3}} \right) & \text{for } m \in \mathcal{M}_1, \\ \Theta(n^\delta) & \text{for } m \in \mathcal{M}_2 \setminus \mathcal{M}_1, \\ \Theta \left( m^{-\frac{2\alpha}{3}} n^{\beta+\delta-\gamma(1-\frac{2\alpha}{3})} \right) & \text{for } m \in \mathcal{M} \setminus \mathcal{M}_2, \end{cases}$$

where  $\mathcal{M}_1 = \{1, \dots, m_1 - 1\}$  and  $\mathcal{M}_2 = \{1, \dots, m_2 - 1\}$ . Here,  $m_1 = \Theta(n^{1-\delta})$  and  $m_2 = \Theta(n^{\gamma-(\gamma-\beta)\frac{3}{2\alpha}})$ .

*Proof:* Refer to Appendix B. □

The optimal solution in Theorem 2 is illustrated in Fig. 3. For  $\alpha \leq \frac{3(\gamma-\beta)}{2(\delta+\gamma-1)}$ , the optimal number of replicas of content object  $m$ ,  $A_m^* + B_m^*$ , is shown to monotonically decrease with  $m$ . For  $\frac{3(\gamma-\beta)}{2(\delta+\gamma-1)} < \alpha < \frac{3}{2}$ , there exists a set of content objects such that  $A_m^* + B_m^*$  scales as  $\Theta(f(n))$ .

Now, we turn to describing our replication strategy by individually choosing the replication sets  $\{A_m^*\}_{m=1}^M$  and

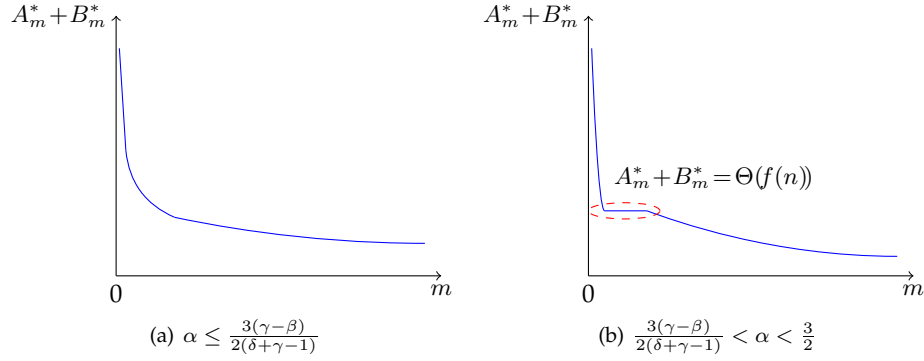


Fig. 3. The optimal cache allocation strategy with respect to the content object  $m$ .

$\{B_m^*\}_{m=1}^M$ . We introduce the following proposition, which exhibits that the resulting  $\{A_m^*\}_{m=1}^M$  and  $\{B_m^*\}_{m=1}^M$  still guarantee the optimality as long as scaling laws are concerned.

**Proposition 1.** Suppose that  $\alpha < \frac{3}{2}$  and the content delivery routing in Section 3 is used for the content-centric mobile hybrid network. Then, the optimal individual replication sets  $\{A_m^*\}_{m=1}^M$  and  $\{B_m^*\}_{m=1}^M$  are given by

$$A_m^* = \begin{cases} \Theta\left(m^{-\frac{2\alpha}{3}} n^{\min\{\beta+\delta-\gamma(1-\frac{2\alpha}{3}), \delta+(1-\delta)\frac{2\alpha}{3}\}}\right) & \text{for } m \in \mathcal{M}_1 \cap \mathcal{M}_2, \\ 0 & \text{for } m \in \mathcal{M} \setminus (\mathcal{M}_1 \cap \mathcal{M}_2) \end{cases} \quad (17)$$

and

$$B_m^* = \begin{cases} \Theta(n^\delta) & \text{for } m \in \mathcal{M}_2, \\ \Theta\left(m^{-\frac{2\alpha}{3}} n^{\beta+\delta-\gamma(1-\frac{2\alpha}{3})}\right) & \text{for } m \in \mathcal{M} \setminus \mathcal{M}_2, \end{cases}$$

respectively, where  $\mathcal{M}_1 = \{1, \dots, m_1 - 1\}$  and  $\mathcal{M}_2 = \{1, \dots, m_2 - 1\}$ . Here,  $m_1 = \Theta(n^{1-\delta})$  and  $m_2 = \Theta(n^{\gamma-(\gamma-\beta)\frac{3}{2\alpha}})$ .

*Proof:* We prove the proposition by individually selecting  $\{A_m^*\}_{m=1}^M$  and  $\{B_m^*\}_{m=1}^M$  that satisfy the optimal solution  $\{A_m^* + B_m^*\}_{m=1}^M$  in Theorem 2 according to the following two cases depending on the value of  $\alpha$ .

Let us first focus on the case where  $\alpha \leq \frac{3(\gamma-\beta)}{2(\delta+\gamma-1)}$ . For  $m \in \mathcal{M}_2$  where  $A_m^* + B_m^* = \Omega(f(n)) (= \Omega(n^\delta))$ , we set  $A_m^* = \Theta\left(m^{-\frac{2\alpha}{3}} n^{\beta+\delta-\gamma(1-\frac{2\alpha}{3})}\right)$  and  $B_m^* = \Theta(n^\delta)$ . For  $\mathcal{M} \setminus \mathcal{M}_2$  where  $A_m^* + B_m^* = o(f(n))$ , we set  $A_m^* = 0$  and  $B_m^* = \Theta\left(m^{-\frac{2\alpha}{3}} n^{\beta+\delta-\gamma(1-\frac{2\alpha}{3})}\right)$ .

Next, we consider the case where  $\frac{3(\gamma-\beta)}{2(\delta+\gamma-1)} < \alpha < \frac{3}{2}$ . For  $m \in \mathcal{M}_1$  where  $A_m^* + B_m^* = \Theta(A_m^*)$ , we set  $A_m^* = \Theta\left(m^{-\frac{2\alpha}{3}} n^{\delta+(1-\delta)\frac{2\alpha}{3}}\right)$  and  $B_m^* = \Theta(n^\delta)$ . For  $m \in \mathcal{M}_2 \setminus \mathcal{M}_1$  where  $A_m^* + B_m^* = \Theta(f(n))$ , we set  $A_m^* = 0$  and  $B_m^* = \Theta(n^\delta)$ . As in the previous case, we also set  $A_m^* = 0$  and  $B_m^* = \Theta\left(m^{-\frac{2\alpha}{3}} n^{\beta+\delta-\gamma(1-\frac{2\alpha}{3})}\right)$  for  $m \in \mathcal{M} \setminus \mathcal{M}_2$ .

From the fact that  $m_1 = \Theta(n^{1-\delta})$  and  $m_2 = \Theta(n^{\gamma-(\gamma-\beta)\frac{3}{2\alpha}})$ , it follows that  $\mathcal{M}_1 \cap \mathcal{M}_2 = \mathcal{M}_2$  if  $\alpha \leq \frac{3(\gamma-\beta)}{2(\delta+\gamma-1)}$ . Otherwise,  $\mathcal{M}_1 \cap \mathcal{M}_2 = \mathcal{M}_1$ . As a consequence, according to the above setting,  $A_m^*$  can be written in a single expression in (17). This completes the proof of the proposition.  $\square$

The optimal replication strategy in Proposition 1 is illustrated in Fig. 4. From this result, the following insightful observations are made.

**Remark 2.** From Fig. 4, it is observed that highly popular content objects, whose number of replicas is  $\omega(f(n))$ , are mainly served by node-to-node multihop routing while the rest of the content objects are served by deployed SBSs. More specifically, from Proposition 1, caching content objects  $m \in \mathcal{M}_1 \cap \mathcal{M}_2$  mostly at mobile nodes is optimal in terms of throughput-delay trade-off. Thus, this replication strategy sheds light on how to cache in large-scale content-centric mobile hybrid networks.

From Theorems 1 and 2 and Proposition 1, we characterize the optimal throughput-delay trade-off. To be specific, the objective function in (8a) is given by

$$\sum_{m=1}^M \frac{p_m}{\sqrt{A_m^* + B_m^*}} = \Theta\left(\frac{n^{\gamma(\frac{3}{2}-\alpha)-\frac{\beta+\delta}{2}}}{H_\alpha(M)}\right),$$

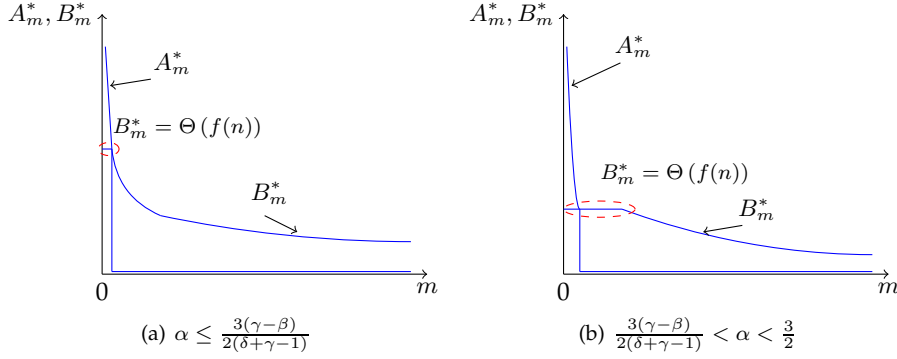


Fig. 4. The replication sets  $\{A_m^*\}_{m=1}^M$  and  $\{B_m^*\}_{m=1}^M$  with respect to the content object  $m$ .

where  $H_\alpha(M) = \sum_{i=1}^M i^{-\alpha}$ . For  $\frac{3(\gamma-\beta)}{2(\delta+\gamma-1)} < \alpha < \frac{3}{2}$ , we have

$$\begin{aligned}
 & \sum_{m=1}^M \frac{p_m}{\sqrt{A_m^* + B_m^*}} \\
 &= \sum_{m=1}^{m_1-1} \frac{p_m}{\sqrt{A_m^* + B_m^*}} + \sum_{m=m_1}^{m_2-1} \frac{p_m}{\sqrt{A_m^* + B_m^*}} + \sum_{m=m_2}^M \frac{p_m}{\sqrt{A_m^* + B_m^*}} \\
 &= \Theta\left(\frac{n^{(1-\delta)(\frac{3}{2}-\alpha)-\frac{1}{2}}}{H_\alpha(M)}\right) + \Theta\left(\frac{n^{-\frac{\delta}{2}} \max\{H_\alpha(m_1), H_\alpha(m_2)\}}{H_\alpha(M)}\right) \\
 &\quad + \Theta\left(\frac{n^{\gamma(\frac{3}{2}-\alpha)-\frac{\beta+\delta}{2}}}{H_\alpha(M)}\right). \tag{18}
 \end{aligned}$$

Let the first, second, and third terms in the right-hand side of (18) be denoted by  $F_1$ ,  $F_2$ , and  $F_3$ , respectively. Then, it is seen that  $F_2 = \Theta(F_1)$  for  $1 < \alpha < \frac{3}{2}$  and  $F_2 = O(F_3)$  for  $\alpha \leq 1$ . In addition, for  $\alpha \leq \frac{3(\gamma-\beta)}{2(\delta+\gamma-1)}$ , the objective function  $\sum_{m=1}^M \frac{p_m}{\sqrt{A_m^* + B_m^*}}$  in (8a) is shown to scale as  $F_3$ . Thus, we need to compare the relative size of  $F_1$  and  $F_3$  according to the four scaling parameters  $\alpha$ ,  $\delta$ ,  $\beta$ , and  $\gamma$  to scrutinize the scaling behavior of (8a). In our work, we partition the entire parameter space, including the case where  $\alpha \geq \frac{3}{2}$ , into three operating regimes as follows (refer to Fig. 5).

- Regime I:  $\{\alpha \mid \alpha \geq \frac{3}{2}\}$
- Regime II:  $\left\{\alpha \mid 1 + \frac{\gamma-\beta}{2(\gamma+\delta-1)} \leq \alpha < \frac{3}{2}\right\}$
- Regime III:  $\left\{\alpha \mid \alpha < 1 + \frac{\gamma-\beta}{2(\gamma+\delta-1)}\right\}$

We are now ready to characterize the optimal throughput-delay trade-off in the following theorem.

**Theorem 3.** Suppose that the content delivery routing in Section 3 and the optimal replication strategy in Proposition 1 are used for the content-centric mobile hybrid network. Then, according to the Zipf exponent  $\alpha$  and the scaling parameters  $\gamma$ ,  $\delta$ , and  $\beta$ , the optimal throughput-delay trade-off is given by

$$\lambda(n) = \Theta\left(\frac{D(n)}{n^b}\right), \text{ where } \lambda(n) = O\left(\frac{1}{\sqrt{n^{b+\epsilon}}}\right),$$

for an arbitrarily small constant  $\epsilon > 0$ . Here,

$$b = \begin{cases} 0 & \text{in Regime I,} \\ (1-\delta)(3-2\alpha) & \text{in Regime II,} \\ 1-\delta-\beta+\min\{3-2\alpha, 1\}\gamma & \text{in Regime III.} \end{cases}$$

*Proof.* In Regime I,  $\lambda(n) = \Theta(D(n))$  is achieved. In Regime II, it is shown that (8a) scales as  $F_1 = \Theta\left(n^{(1-\delta)(\frac{3}{2}-\alpha)-\frac{1}{2}}\right)$ , thereby resulting in  $b = (1-\delta)(3-2\alpha)$  from (5). Now, let us turn to Regime III as follows: for  $1 < \alpha < 1 + \frac{\gamma-\beta}{2(\gamma+\delta-1)}$ , (8a) scales as  $F_3 = \Theta\left(n^{\gamma(\frac{3}{2}-\alpha)-\frac{\beta+\delta}{2}}\right)$ ; and for  $\alpha \leq 1$ , (8a) scales as  $F_3 = \Theta\left(n^{\frac{\gamma}{2}-\frac{\delta+\beta}{2}}\right)$ . Thus, we have  $b = 1-\delta-\beta+\min\{3-2\alpha, 1\}$ . This completes the proof of the theorem.  $\square$

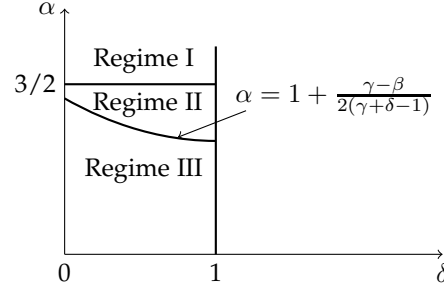


Fig. 5. The operating regimes on the throughput–delay trade-off with respect to  $\alpha$ ,  $\delta$ ,  $\beta$ , and  $\gamma$ .

TABLE 1  
The simulation environment

Symbol	Description	Value
$n$	The number of mobile nodes	300
$M$	The size of the library	200
$f(n)$	The number of SBSs	50
$K_{SBS}$	The cache size of each SBS	50
$K_n$	The cache size of each node	2

The impact and benefits of SBSs equipped with a finite-size cache are explicitly addressed according to each operating regime on the optimal throughput–delay trade-off.

**Remark 3.** *In Regime I, the best performance  $\lambda(n) = \Theta(D(n))$  is achieved by using node-to-node multihop communication, and thus the use of SBSs does not further improve the performance. On the other hand, in Regimes II and III, it turns out that the supplemental cache space  $f(n)K_{SBS}$  in the mobile hybrid network significantly improves the network performance over the mobile ad hoc network with no SBS. Interestingly, in Regime II, the optimal trade-off is shown to be the same as in the content-centric static hybrid network case assuming BSs equipped with the infinite-size cache (or equivalently, the infinite-speed backhaul-aided cache) [22], [23].*

### 5.3 Numerical Evaluation

In this subsection, to validate the analytical results shown in Section 5.2, we perform intensive numerical evaluation by numerically solving the optimization problem in (8) according to finite values of the system parameters  $n$ ,  $M$ ,  $K_n$ ,  $K_{SBS}$ , and  $f(n)$  in TABLE 1, where the exponents  $\gamma$ ,  $\beta$ , and  $\delta$  are given by 0.93, 0.69, and 0.69, respectively. As in Section 5.2, we consider two cases  $\alpha \leq \frac{3(\gamma-\beta)}{2(\delta+\gamma-1)}$  and  $\frac{3(\gamma-\beta)}{2(\delta+\gamma-1)} < \alpha < \frac{3}{2}$ , where  $\frac{3(\gamma-\beta)}{2(\delta+\gamma-1)} = 0.59$ . To account for a distinct feature of the optimal solution to (8) in each case, the following two values of  $\alpha$  are used:  $\alpha = 0.55$  and  $\alpha = 1.2$ .

In Fig. 6, the set  $\{A_m^* + B_m^*\}_{m=1}^{200}$  is illustrated according to the content object  $m$ . It is found that the simulation results are consistent with our analytical trend in Theorem 2, which is depicted in Fig. 3. More specifically, for  $\alpha = 0.55$ , it is shown in Fig. 6(a) that  $A_m^* + B_m^*$  monotonically decreases as  $m$  increases. Besides, as illustrated in Fig. 6(b), there exists a set of content objects  $m$  such that  $A_m^* + B_m^*$  is approximately given by  $f(n) = 50$  for  $\alpha = 1.2$ .

In Fig. 7, the sets  $\{A_m^*\}_{m=1}^{200}$  and  $\{B_m^*\}_{m=1}^{200}$  are illustrated according to  $m$ . It is also found that the overall trends in the figure are similar to our analytical result in Proposition 1, which is depicted in Fig. 4. Our numerical results indicate that only a subset of highly popular content objects are mainly cached and delivered by mobile nodes. It is also observed that  $B_m^*$  is close to  $f(n) = 50$  for small  $m$  and then decreases as  $m$  increases.

## 6 BASELINE STRATEGY IN MOBILE HYBRID NETWORKS

In this section, for comparison, we present a baseline cache allocation strategy, where the replication sets  $\{A_m\}_{m=1}^M$  and  $\{B_m\}_{m=1}^M$  are found by solving two separate optimization problems instead of our original problem in (8). We first present the problem formulation and then find the individual replication sets. Finally, performance comparison is conducted between two cache allocation strategies.

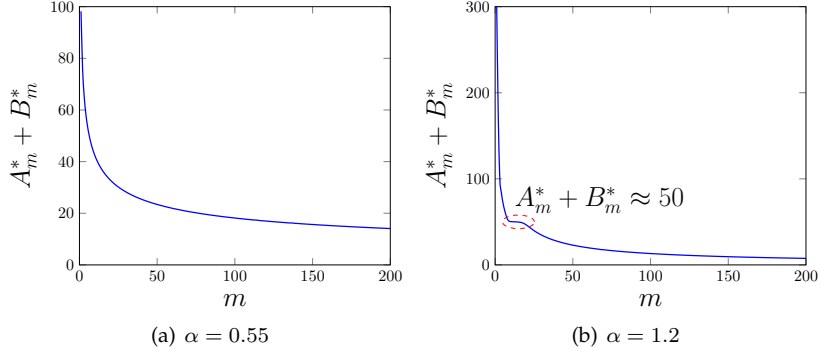


Fig. 6. The optimal set  $\{A_m^* + B_m^*\}_{m=1}^{200}$  with respect to the content object  $m$ .

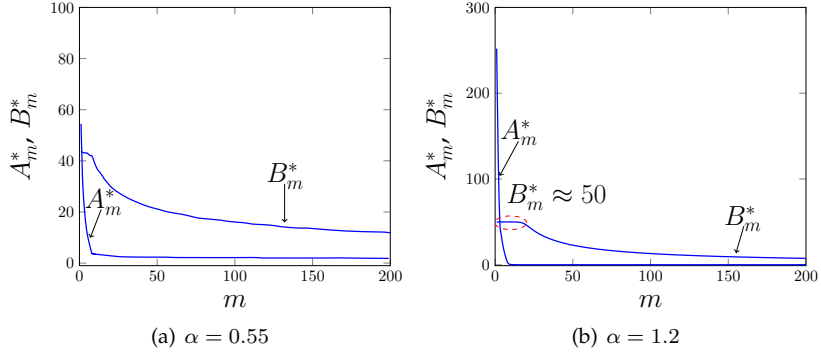


Fig. 7. The proposed individual replication sets  $\{A_m^*\}_{m=1}^{200}$  and  $\{B_m^*\}_{m=1}^{200}$  with respect to the content object  $m$ .

## 6.1 Problem Formulation

For the baseline approach, we consider two scenarios such that all content objects are stored only at mobile nodes (i.e.,  $K_{SBS} = 0$ ) or only at SBSs (i.e.,  $K_n = 0$ ). Then, the objective function (8a) boils down to  $\sum_{m=1}^M \frac{p_m}{\sqrt{A_m}}$  or  $\sum_{m=1}^M \frac{p_m}{\sqrt{B_m}}$ . To be specific, two optimization problems can be formulated as follows:

$$\min_{\{A_m\}_{m=1}^M} \sum_{m=1}^M \frac{p_m}{\sqrt{A_m}} \quad (19a)$$

$$\text{subject to } \sum_{m=1}^M A_m \leq nK_n, \quad (19b)$$

$$1 \leq A_m \leq n \text{ for } m \in \mathcal{M} \quad (19c)$$

and

$$\min_{\{B_m\}_{m=1}^M} \sum_{m=1}^M \frac{p_m}{\sqrt{B_m}} \quad (20a)$$

$$\text{subject to } \sum_{m=1}^M B_m \leq f(n)K_{SBS}, \quad (20b)$$

$$1 \leq B_m \leq f(n) \text{ for } m \in \mathcal{M}. \quad (20c)$$

In the same manner used in Section 5, the discrete variables  $A_m$  and  $B_m$  are relaxed to real number in  $[1, \infty)$  to preserve the convexity of the objective functions (19a) and (20a).

## 6.2 Analytical Results

As in Section 5.2, we use the Lagrangian relaxation method for solving two optimization problems in (19) and (20). We establish the following theorem, which characterizes the optimal total number of replicas of content object  $m \in \mathcal{M}$ .

**Theorem 4.** Suppose that  $\alpha < 3/2$  and the content delivery routing in Section 3 is used for the content-centric mobile hybrid network. Then, the optimal solutions to (19) and (20) lead to

$$A_m^* + B_m^* = \begin{cases} \Theta\left(m^{-\frac{2\alpha}{3}} n^{1-\gamma(1-\frac{2\alpha}{3})}\right) & \text{for } m \in \mathcal{M}_4, \\ \Theta(n^\delta) & \text{for } m \in \mathcal{M}_2 \setminus \mathcal{M}_4, \\ \Theta\left(m^{-\frac{2\alpha}{3}} n^{\beta+\delta-\gamma(1-\frac{2\alpha}{3})}\right) & \text{for } m \in \mathcal{M} \setminus \mathcal{M}_2, \end{cases}$$

where  $\mathcal{M}_2 = \{1, \dots, m_2 - 1\}$  and  $\mathcal{M}_4 = \{1, \dots, m_4 - 1\}$ . Here,  $m_2 = \Theta\left(n^{\gamma-(\gamma-\beta)\frac{3}{2\alpha}}\right)$  and  $m_4 = \Theta\left(n^{\gamma-(\gamma+\delta-1)\frac{3}{2\alpha}}\right)$ .

*Proof:* Since the first problem (19) corresponds to the optimization problem for the ad hoc network case with no SBS, the optimal replication set  $\{A_m^*\}_{m=1}^M$  is given by

$$A_m^* = \Theta\left(m^{-\frac{2\alpha}{3}} n^{1-\gamma(1-\frac{2\alpha}{3})}\right) \quad (21)$$

for  $\alpha < \frac{3}{2}$  [22], [23].

Now, let us turn to solving the second problem (20), which corresponds to the scenario where content objects are stored only at SBSs. Using arguments similar to those in the proof of Theorem 2, it is not difficult to derive that  $B_m^* = \Theta(f(n)) = \Theta(n^\delta)$  for  $m \in \mathcal{M}_2 \triangleq \{1, \dots, m_2 - 1\}$  and

$$B_m^* = \Theta\left(m^{-\frac{2\alpha}{3}} n^{\beta+\delta-\gamma(1-\frac{2\alpha}{3})}\right) \quad (22)$$

for  $m \in \mathcal{M} \setminus \mathcal{M}_2$ , where  $m_2 = \Theta\left(n^{\gamma-(\gamma-\beta)\frac{3}{2\alpha}}\right)$ .

From (21) and (22), we next focus on deciding when each replication set  $A_m^*$  or  $B_m^*$  is dominant for all  $m \in \mathcal{M}$ . Under the given condition that  $\delta + \beta \geq 1$ , we have  $B_m^* = \Omega(A_m^*)$  for  $m \in \mathcal{M} \setminus \mathcal{M}_2$ . Let  $\mathcal{M}_4 \triangleq \{1, \dots, m_4 - 1\}$  denote the set of content objects such that  $A_m^* + B_m^* = \Theta(A_m^*)$  under our baseline strategy, where  $m_4 - 1$  is the largest index of the set  $\mathcal{M}_4$ . Then, using (21) and the fact that  $A_{m_4-1}^* = \Theta(B_{m_4-1}^*) = \Theta(n^\delta)$ , we have  $n^\delta = \Theta\left(m_4^{-\frac{2\alpha}{3}} n^{1-\gamma(1-\frac{2\alpha}{3})}\right)$ , which results in  $m_4 = \Theta\left(n^{\gamma-(\gamma+\delta-1)\frac{3}{2\alpha}}\right)$ . This completes the proof of the theorem.  $\square$

Now, the above baseline strategy is compared with the optimal one in Section 5. The throughput-delay trade-off of the baseline strategy can be found by applying the result in Theorem 4 to the objective function (8a). As a consequence, we have

$$\begin{aligned} & \sum_{m=1}^M \frac{p_m}{\sqrt{A_m^* + B_m^*}} \\ &= \sum_{m=1}^{m_4-1} \frac{p_m}{\sqrt{A_m^* + B_m^*}} + \sum_{m=m_4}^{m_2-1} \frac{p_m}{\sqrt{A_m^* + B_m^*}} + \sum_{m=m_2}^M \frac{p_m}{\sqrt{A_m^* + B_m^*}} \\ &= \Theta\left(\frac{n^{(\gamma-(\gamma+\delta-1)\frac{1}{\alpha})(\frac{3}{2}-\alpha)-\frac{1}{2}}}{H_\alpha(M)}\right) \\ &+ \Theta\left(\frac{n^{-\frac{\delta}{2}} \max\{H_\alpha(m_2), H_\alpha(m_4)\}}{H_\alpha(M)}\right) + \Theta\left(\frac{n^{\gamma(\frac{3}{2}-\alpha)-\frac{\beta+\delta}{2}}}{H_\alpha(M)}\right). \end{aligned} \quad (23)$$

Let the first, second, and third terms in the right-hand side of (23) be denoted by  $F_4$ ,  $F_5$ , and  $F_3$ , respectively. Then, it is seen that  $F_5 = \Theta(F_4)$  for  $1 < \alpha < \frac{3}{2}$  and  $F_5 = O(F_3)$  for  $\alpha \leq 1$ . Thus, by comparing the relative size of  $F_3$  and  $F_4$ , one can show that if  $\frac{3(\gamma+\delta-1)}{3(\gamma+\delta-1)-(\gamma-\beta)} \leq \alpha < \frac{3}{2}$ , then  $F_4 = \Omega(F_3)$ ; and  $F_4 = o(F_3)$  otherwise. Next, for comparison with the optimal strategy in Section 5, we take into account the following three cases according to the values of  $\alpha$ . For  $\alpha < \frac{3(\gamma+\delta-1)}{3(\gamma+\delta-1)-(\gamma-\beta)}$ , the objective function (8a) scales as  $F_3$ , which implies that both optimal and baseline strategies have the same throughput-delay trade-off. For  $\frac{3(\gamma+\delta-1)}{3(\gamma+\delta-1)-(\gamma-\beta)} \leq \alpha < 1 + \frac{\gamma-\beta}{2(\gamma+\delta-1)}$  and  $1 + \frac{\gamma-\beta}{2(\gamma+\delta-1)} \leq \alpha < \frac{3}{2}$ , (8a) scales as  $F_3$  and  $F_1$ , respectively, under the optimal strategy, while it scales as  $F_4$  under the baseline. Since  $F_4$  is greater than both  $F_3$  and  $F_1$  in these two cases, the optimal one provides a better throughput-delay trade-off for  $\frac{3(\gamma+\delta-1)}{3(\gamma+\delta-1)-(\gamma-\beta)} \leq \alpha < \frac{3}{2}$ . Therefore, the baseline cache allocation strategy is strictly suboptimal.

**Remark 4.** The performance gain over the baseline approach basically comes from the fact that in our optimal cache allocation strategy, mobile nodes can further cache highly popular content objects, whose number of replicas is larger than the number of SBSs. This finally leads to the performance improvement in terms of throughput-delay trade-off when  $A_m^* + B_m^* = \omega(n^\delta)$ .

Note that for  $\alpha \geq \frac{3}{2}$  (corresponding to the case where the use of SBSs is not beneficial), the objective function (8a) scales as  $\frac{1}{\sqrt{n}}$  when the baseline strategy is used, which also exhibits the best throughput–delay trade-off in our mobile hybrid network from the result of Theorem 1.

## 7 CONCLUDING REMARKS

This paper analyzed the optimal throughput–delay trade-off in content-centric mobile hybrid networks, where each of mobile nodes and static SBSs is equipped with a finite cache size. A content delivery routing was first proposed to characterize a fundamental throughput–delay trade-off. Then, the optimal cache allocation strategy, which jointly finds the number of replicas cached at mobile nodes and SBSs using a variable decoupling technique, was presented to achieve the optimal throughput–delay trade-off. Our analytical results were comprehensively validated by numerical evaluation.

Suggestions for further research includes characterizing the optimal throughput–delay trade-off in mobile hybrid networks for the case where the size of each content object is considerably large and thus the per-hop time required for content delivery may be greater than the duration of each time slot.

## APPENDIX A

### PROOF OF LEMMA 2

Let us first prove that  $A_m^*$  is non-increasing with  $m \in \mathcal{M}_1$ . From (12), we have

$$-\frac{p_m}{2\sqrt{A_m^{*3}}} + \lambda^* + w_m^* = 0 \text{ for } m \in \mathcal{M}_1. \quad (\text{A.1})$$

Let  $\mathcal{D}_1 \subset \mathcal{M}_1$  denote the set of content objects such that  $A_m^* = n$  and  $m_0$  denote the smallest index such that  $A_{m_0}^* < n$ . Now, consider any content object  $k \in \mathcal{D}_1$ . Then, using (A.1) and the fact that  $w_{m_0}^* = 0$ , we have  $\lambda^* = \frac{p_k}{2\sqrt{A_k^{*3}}} - w_k^* = \frac{p_{m_0}}{2\sqrt{A_{m_0}^{*3}}} > 0$ . Since  $A_k^* = n$ ,  $A_{m_0}^* < n$ , and  $w_k^* \geq 0$ , we obtain  $p_k > p_{m_0}$ , thus resulting in  $k < m_0$  due to the feature of a Zipf popularity in (1). That is,  $\mathcal{D}_1 = \{1, 2, \dots, m_0 - 1\}$ . Furthermore, for  $m \in \mathcal{M}_1 \setminus \mathcal{D}_1$ , using (13) and (A.1), we have  $A_m^* = \frac{p_m^{\frac{2}{3}}}{(2\lambda^*)^{\frac{2}{3}}}$ , which decreases with  $m$ . Therefore,  $A_m^*$  is non-increasing with  $m \in \mathcal{M}_1$ .

Let us turn to proving that  $B_m^*$  is non-increasing with  $m \in \mathcal{M}_3$ . Let  $\mathcal{D}_2 \subset \mathcal{M}_3$  denote the set of content objects such that  $B_m^* = f(n)$  and  $\tilde{m}_0$  denote the smallest index such that  $B_{\tilde{m}_0}^* < f(n)$ . By applying the KKT conditions for (10) and the same approach as above, one can show that  $\mathcal{D}_2 = \{1, 2, \dots, \tilde{m}_0 - 1\}$  and  $B_m^* = \frac{p_{\tilde{m}}^{\frac{2}{3}}}{(2\mu^*)^{\frac{2}{3}}}$  for  $m \in \mathcal{M}_3 \setminus \mathcal{D}_2$ , which decreases with  $m$ . Therefore,  $B_m^*$  is non-increasing with  $m \in \mathcal{M}_3$ . This completes the proof of the lemma.

## APPENDIX B

### PROOF OF THEOREM 2

As shown in the proof of Lemma 2 (see Appendix A), applying the KKT conditions for (9) and (10), we have

$$A_m^* = \frac{p_m^{\frac{2}{3}}}{(2\lambda^*)^{\frac{2}{3}}} \text{ for } m \in \mathcal{M}_1 \setminus \mathcal{D}_1 \quad (\text{B.2})$$

and

$$B_m^* = \frac{p_{\tilde{m}}^{\frac{2}{3}}}{(2\mu^*)^{\frac{2}{3}}} \text{ for } m \in \mathcal{M}_3 \setminus \mathcal{D}_2, \quad (\text{B.3})$$

where  $\mathcal{D}_1 \subset \mathcal{M}_1$  and  $\mathcal{D}_2 \subset \mathcal{M}_3$  are the sets of content objects such that  $A_m^* = n$  and  $B_m^* = f(n)$ , respectively. From the proof of Lemma 2, recall that  $\mathcal{D}_1 = \{1, \dots, m_0 - 1\}$ , where  $m_0$  denotes the smallest index such that  $A_m^* < n$ . Using (14) and (16), one can show that  $\sum_{m=1}^M A_m^* = nK_n$  and  $\sum_{m=1}^M B_m^* = f(n)K_{SBS}$  due to the fact that  $\lambda^* > 0$  and  $\mu^* > 0$ , respectively, which will be used for computing the sum of  $A_m^* + B_m^*$  over some indices in  $\mathcal{M}$ .

The optimization problem (8) can be solved according to the following two cases depending on how the Lagrangian multiplier  $\lambda^*$  in (11) scales with the another one  $\mu^*$  in (15). In particular, we consider two cases where  $\lambda^* = \Theta(\mu^*)$  and  $\lambda^* \neq \Theta(\mu^*)$ , each of which corresponds to the cases where  $\alpha \leq \frac{3(\gamma-\beta)}{2(\delta+\gamma-1)}$  and  $\frac{3(\gamma-\beta)}{2(\delta+\gamma-1)} < \alpha < \frac{3}{2}$ .

**Case 1:** We first consider the case where  $\lambda^* = \Theta(\mu^*)$ . Using (B.2) and (B.3), one can show that  $A_m^* + B_m^*$  is computed as

$$A_m^* + B_m^* = \frac{p_m^{\frac{2}{3}}}{\xi^{\frac{2}{3}}}, \quad (\text{B.4})$$

where  $\xi = \Theta(\lambda^*) = \Theta(\mu^*)$  for  $\forall m \in \mathcal{M} \setminus \mathcal{D}_1$ . By adding up  $A_m^* + B_m^*$  in (B.4) over  $\forall m \in \mathcal{M} \setminus \mathcal{D}_1$  and using the fact that  $\xi^{\frac{2}{3}} = \frac{\sum_{l=m_0}^M p_l^{\frac{2}{3}}}{\sum_{l=m_0}^M (A_l^* + B_l^*)}$ , we obtain

$$\begin{aligned} A_m^* + B_m^* &= \frac{p_m^{\frac{2}{3}}}{\sum_{l=m_0}^M p_l^{\frac{2}{3}}} \sum_{l=m_0}^M (A_l^* + B_l^*) \\ &= \Theta\left(m^{-\frac{2\alpha}{3}} n^{\beta+\delta-\gamma(1-\frac{2\alpha}{3})}\right). \end{aligned} \quad (\text{B.5})$$

Here, the second equality holds since the cardinality of  $\mathcal{D}_1$  is  $O(1)$  due to the cache space  $K_n = \Theta(1)$ ;  $\sum_{l=m_0}^M (A_l^* + B_l^*) = \Theta(n^{\delta+\beta})$  from the assumption that  $\delta + \beta \geq 1$  as  $K_{SBS} = \Theta(n^\beta)$  and  $f(n) = \Theta(n^\delta)$ ; from (1) and (2),  $\sum_{l=m_0}^M p_l^{\frac{2}{3}} = \sum_{l=m_0}^M \frac{l^{-\frac{2\alpha}{3}}}{H_\alpha^{\frac{2}{3}}(M)} = \Theta\left(\frac{M^{1-\frac{2\alpha}{3}}}{H_\alpha^{\frac{2}{3}}(M)}\right)$  for  $\alpha < \frac{3}{2}$ ; and  $M = \Theta(n^\gamma)$ .

Now, we proceed with proving that the set  $\mathcal{D}_1$  does not exist by contradiction. Suppose that there exists  $\mathcal{D}_1$  (or equivalently  $m_0 > 1$ ). When the largest index in the set  $\mathcal{M}_2$  of content objects such that  $A_m^* + B_m^* = \Omega(f(n))$  is denoted as  $m_2 - 1$ , it follows that  $A_{m_2-1}^* + B_{m_2-1}^* = \Theta(f(n))$ . Using (B.5), we have  $f(n) = \Theta\left((m_2 - 1)^{-\frac{2\alpha}{3}} n^{\beta+\delta-\gamma(1-\frac{2\alpha}{3})}\right)$ , which then yields

$$m_2 = \Theta\left(n^{\gamma-(\gamma-\beta)\frac{3}{2\alpha}}\right). \quad (\text{B.6})$$

Meanwhile, it is seen that  $\mathcal{M}_1 \setminus \mathcal{D}_1 = \{m_0, \dots, m_2 - 1\}$ . This is because the set  $\mathcal{M}_2$  belongs to  $\mathcal{M}_1$  from the fact that  $B_m^* \leq f(n)$ . By adding up  $A_m^* + B_m^*$  in (B.4) over all  $m \in \mathcal{M}_1 \setminus \mathcal{D}_1$ , we thus have

$$A_m^* + B_m^* = \Theta(A_m^*) = \frac{p_m^{\frac{2}{3}}}{\sum_{l=m_0}^{m_2-1} p_l^{\frac{2}{3}}} \sum_{l=m_0}^{m_2-1} \Theta(A_l^*),$$

which results in

$$A_{m_0}^* = \Theta\left(\frac{\sum_{l=m_0}^{m_2-1} A_l^*}{(m_2 - 1)^{1-\frac{2\alpha}{3}}}\right) \quad (\text{B.7})$$

when  $m = m_0$  due to the fact that from (1) and (2),  $\sum_{l=m_0}^{m_2-1} p_l^{\frac{2}{3}} = \sum_{l=m_0}^{m_2-1} \frac{l^{-\frac{2\alpha}{3}}}{H_\alpha^{\frac{2}{3}}(M)} = \Theta\left(\frac{(m_2 - 1)^{1-\frac{2\alpha}{3}}}{H_\alpha^{\frac{2}{3}}(M)}\right)$  for  $\alpha < \frac{3}{2}$ . Since  $(m_2 - 1)^{1-\frac{2\alpha}{3}} = \omega(1)$  from (B.6) and  $\sum_{l=m_0}^{m_2-1} A_l^* = O(n)$ , it follows that  $A_{m_0}^* = o(n)$  from (B.7), which contradicts another relation  $A_{m_0}^* = \Theta(n)$ . Hence, we conclude that  $\mathcal{D}_1$  does not exist (i.e.,  $m_0 = 1$ ).

In the following, we show that the condition  $\lambda^* = \Theta(\mu^*)$  is identical to  $\alpha \leq \frac{3(\gamma-\beta)}{2(\delta+\gamma-1)}$ . Using (B.5) and (B.6) as well as  $m_0 = 1$ , we have  $\sum_{m=1}^{m_2-1} (A_m^* + B_m^*) = \frac{\sum_{m=1}^{m_2-1} p_m^{\frac{2}{3}}}{\sum_{l=1}^M p_l^{\frac{2}{3}}} \sum_{l=1}^M (A_l^* + B_l^*) = \Theta\left(n^{\delta+\beta-(\gamma-\beta)(\frac{3}{2\alpha}-1)}\right)$ . Using the fact that  $\sum_{m=1}^{m_2-1} (A_m^* + B_m^*) = \sum_{m=1}^{m_2-1} \Theta(A_m^*) = O(n)$ , we obtain the following inequality:  $\delta + \beta - (\gamma - \beta)(\frac{3}{2\alpha} - 1) \leq 1$ , which is equivalent to  $\alpha \leq \frac{3(\gamma-\beta)}{2(\delta+\gamma-1)}$ . Therefore, if  $\alpha \leq \frac{3(\gamma-\beta)}{2(\delta+\gamma-1)}$ , then

$$A_m^* + B_m^* = \Theta\left(m^{-\frac{2\alpha}{3}} n^{\beta+\delta-\gamma(1-\frac{2\alpha}{3})}\right) \text{ for } m \in \mathcal{M}.$$

**Case 2:** We turn our attention to the case where  $\lambda^* \neq \Theta(\mu^*)$ . From (B.2) and (B.3), it is found that the two sets  $\mathcal{M}_1 \setminus \mathcal{D}_1$  and  $\mathcal{M}_3 \setminus \mathcal{D}_2$  do not share any common content object. Thus, it follows that  $\mathcal{M}_1 \subset \mathcal{M}_2$ . Based on this observation, we have

$$A_m^* + B_m^* = \Theta(B_m^*) = \Theta\left(n^\delta\right) \quad (\text{B.8})$$

for  $m \in \mathcal{M}_2 \setminus \mathcal{M}_1$ . For the sake of analytical convenience, by defining  $m_1 - 1$  and  $m_2 - 1$  as the largest indices in the sets  $\mathcal{M}_1$  and  $\mathcal{M}_2$ , respectively, we compute  $A_m^* + B_m^*$  for  $m \in \mathcal{M}_1$  and  $m \in \mathcal{M} \setminus \mathcal{M}_2$ .

First, we focus on finding both  $A_m^* + B_m^*$  and  $m_2$  for  $m \in \mathcal{M} \setminus \mathcal{M}_2$ , where  $\mathcal{M} \setminus \mathcal{M}_2 = \{m_2, \dots, M\}$ . By adding up  $B_m^*$

in (B.3) over all  $m \in \mathcal{M} \setminus \mathcal{M}_2$ , we have

$$B_m^* = \frac{p_m^{\frac{2}{3}}}{\sum_{l=m_2}^M p_l^{\frac{2}{3}}} \sum_{l=m_2}^M B_l^* \quad (\text{B.9a})$$

$$= O\left(m^{-\frac{2\alpha}{3}} n^{\delta+\beta-\gamma(1-\frac{2\alpha}{3})}\right), \quad (\text{B.9b})$$

where the second equality holds since  $\sum_{l=m_2}^M B_l^* = O(n^{\delta+\beta})$ ; from (1) and (2),  $\sum_{l=m_2}^M p_l^{\frac{2}{3}} = \sum_{l=m_2}^M \frac{l^{-\frac{2\alpha}{3}}}{H_\alpha^{\frac{2}{3}}(M)} = \Theta\left(\frac{M^{1-\frac{2\alpha}{3}}}{H_\alpha^{\frac{2}{3}}(M)}\right)$  for  $\alpha < \frac{3}{2}$ ; and  $M = \Theta(n^\gamma)$ . From (B.9b) and  $B_{m_2}^* = \Theta(f(n))$ , we have  $f(n) = O\left(m_2^{-\frac{2\alpha}{3}} n^{\delta+\beta-\gamma(1-\frac{2\alpha}{3})}\right)$ , which leads to  $m_2 = O\left(n^{\gamma-(\gamma-\beta)\frac{3}{2\alpha}}\right)$ . Since  $(\gamma - \beta)(1 - \frac{3}{2\alpha}) < 0$  under our network model, it follows that  $\gamma - (\gamma - \beta)\frac{3}{2\alpha} < \beta$ , thus resulting in  $m_2 = o(K_{SBS})$ . Because  $\sum_{l=m_2}^M B_l^* = f(n)K_{SBS} - O(m_2 f(n)) = \Theta(n^{\delta+\beta})$ , (B.9a) can be rewritten as

$$A_m^* + B_m^* = \Theta(B_m^*) = \Theta\left(m^{-\frac{2\alpha}{3}} n^{\delta+\beta-\gamma(1-\frac{2\alpha}{3})}\right) \quad (\text{B.10})$$

for  $m \in \mathcal{M} \setminus \mathcal{M}_2$ . Moreover, using the fact that  $A_{m_2}^* + B_{m_2}^* = \Theta\left(m_2^{-\frac{2\alpha}{3}} n^{\delta+\beta-\gamma(1-\frac{2\alpha}{3})}\right)$  from (B.10) and  $A_{m_2}^* + B_{m_2}^* = \Theta(f(n))$ , we obtain

$$m_2 = \Theta\left(n^{\gamma-(\gamma-\beta)\frac{3}{2\alpha}}\right). \quad (\text{B.11})$$

Next, we turn to finding both  $A_m^* + B_m^*$  and  $m_1$  for  $m \in \mathcal{M}_1$ . By adding up  $A_m^*$  in (B.2) over  $\forall m \in \mathcal{M}_1 \setminus \mathcal{D}_1$  ( $= \{m_0, \dots, m_1 - 1\}$ ), we have

$$A_m^* = \frac{p_m^{\frac{2}{3}}}{\sum_{l=m_0}^{m_1-1} p_l^{\frac{2}{3}}} \sum_{l=m_0}^{m_1-1} A_l^*. \quad (\text{B.12})$$

Similarly as in Case 1, we are capable of proving that  $\mathcal{D}_1$  does not exist (i.e.,  $m_0 = 1$ ). Because  $f(n) = \Theta\left(\frac{m_1^{-\frac{2\alpha}{3}} \sum_{l=1}^{m_1-1} A_l^*}{(m_1-1)^{1-\frac{2\alpha}{3}}}\right)$

due to  $\sum_{l=1}^{m_1-1} p_l^{\frac{2}{3}} = \Theta\left(\frac{(m_1-1)^{1-\frac{2\alpha}{3}}}{H_\alpha^{\frac{2}{3}}(M)}\right)$  and  $A_{m_1-1}^* = \Theta(f(n))$ , it is not difficult to show that

$$m_1 = \Theta\left(\frac{\sum_{l=1}^{m_1-1} A_l^*}{f(n)}\right). \quad (\text{B.13})$$

Now, we need to specify the term  $\sum_{l=1}^{m_1-1} A_l^*$  to find  $m_1$ . For  $\alpha < \frac{3}{2}$ , by setting  $m_0 = 1$ , the objective function (8a) can be expressed as

$$\begin{aligned} & \sum_{m=1}^M \frac{p_m}{\sqrt{A_m^* + B_m^*}} \\ &= \sum_{m=1}^{m_1-1} \frac{p_m}{\sqrt{A_m^* + B_m^*}} + \sum_{m=m_1}^{m_2-1} \frac{p_m}{\sqrt{A_m^* + B_m^*}} + \sum_{m=m_2}^M \frac{p_m}{\sqrt{A_m^* + B_m^*}} \\ &= \Theta\left(\frac{\left(\sum_{m=1}^{m_1-1} p_m^{\frac{2}{3}}\right)^{\frac{3}{2}}}{\sqrt{\sum_{m=1}^{m_1-1} A_m^*}}\right) + \Theta\left(\frac{\sum_{m=m_1}^{m_2-1} p_m}{\sqrt{f(n)}}\right) + \Theta\left(\frac{\left(\sum_{m=m_2}^M p_m^{\frac{2}{3}}\right)^{\frac{3}{2}}}{\sqrt{\sum_{m=m_2}^M B_m^*}}\right) \\ &= \Theta\left(\frac{m_1^{1-\alpha}}{H_\alpha(M)\sqrt{f(n)}}\right) + \Theta\left(\frac{\max\{H_\alpha(m_1), H_\alpha(m_2-1)\}}{H_\alpha(M)\sqrt{f(n)}}\right) \\ & \quad + \Theta\left(\frac{M^{3/2-\alpha}}{H_\alpha(M)\sqrt{f(n)K_{SBS}}}\right), \end{aligned} \quad (\text{B.14})$$

where the second equality follows from (B.8) for  $m \in \mathcal{M}_2 \setminus \mathcal{M}_1$ , (B.9a) for  $m \in \mathcal{M} \setminus \mathcal{M}_2$ , and (B.12) for  $m \in \mathcal{M}_1$ ; the third equality holds since  $m_2 = o(M)$  from (B.11) as well as  $\sum_{l=1}^{m_1-1} p_l^{\frac{2}{3}} = \Theta\left(\frac{(m_1-1)^{1-\frac{2\alpha}{3}}}{H_\alpha^{\frac{2}{3}}(M)}\right)$  and  $\sum_{l=m_2}^M p_l^{\frac{2}{3}} = \Theta\left(\frac{M^{1-\frac{2\alpha}{3}}}{H_\alpha^{\frac{2}{3}}(M)}\right)$  from (1) and (2). One can show that the second term in (B.14) scales slower than the other two terms because for  $\alpha \leq 1$ , (8a) is given by the third term in (B.14) and for  $1 < \alpha < \frac{3}{2}$ , (8a) is dominated by either the first or the third term in (B.14). Since for  $1 < \alpha < \frac{3}{2}$ , the first term (including  $m_1$ ) can be minimized when  $m_1$  is maximized, it follows that  $\sum_{l=1}^{m_1-1} A_l^* = \Theta(n)$

from (3) (the total caching constraint) and (B.13). Accordingly, we have

$$m_1 = \Theta(n^{1-\delta}).$$

Moreover by setting  $m_0 = 1$ ,  $\sum_{l=1}^{m_1-1} p_l^{\frac{2}{3}} = \Theta\left(\frac{m_1^{1-\frac{2\alpha}{3}}}{H_{\alpha}^{\frac{2}{3}}(M)}\right)$ , and  $\sum_{l=1}^{m_1-1} A_l^* = \Theta(n)$ , (B.12) can be rewritten as

$$A_m^* + B_m^* = \Theta(A_m^*) = \Theta\left(m^{-\frac{2\alpha}{3}} n^{\delta+(1-\delta)\frac{2\alpha}{3}}\right) \text{ for } m \in \mathcal{M}_1.$$

As the last case, for  $m \in \mathcal{M}_2 \setminus \mathcal{M}_1$ ,  $A_m^* + B_m^*$  is obviously given by  $\Theta(n^\delta)$  from the definitions of  $\mathcal{M}_1$  and  $\mathcal{M}_2$ .

Finally, from the last paragraph of Case 1, it is obvious that  $\lambda^* \neq \Theta(\mu^*)$  when  $\frac{3(\gamma-\beta)}{2(\delta+\gamma-1)} < \alpha < \frac{3}{2}$ . This completes the proof of the theorem.

## ACKNOWLEDGMENTS

This research was supported by the Basic Science Research Program through the National Research Foundation of Korea (NRF) funded by the Ministry of Education (2017R1D1A1A09000835) and by the Ministry of Science, ICT & Future Planning (MSIP) (2015R1A2A1A15054248). The material in this paper was presented in part at the IEEE International Symposium on Information Theory, Barcelona, Spain, July 2016 [30].

## REFERENCES

- [1] "Cisco visual networking index: Global mobile data traffic forecast update, 2015-2020," *Cisco Public Information*, Feb. 2016.
- [2] V. Jacobson, D. K. Smetters, J. D. Thornton, M. F. Plass, N. H. Briggs, and R. L. Braynard, "Networking named content," *Commun. ACM*, vol. 55, no. 1, pp. 117–124, Jan. 2012.
- [3] M. Ji, G. Caire, and A. F. Molisch, "Wireless device-to-device caching networks: Basic principles and system performance," *IEEE J. Sel. Areas Commun.*, vol. 34, no. 1, pp. 176–189, Jan. 2016.
- [4] P. Gupta and P. R. Kumar, "The capacity of wireless networks," *IEEE Trans. Inf. Theory*, vol. 46, no. 2, pp. 388–404, Mar. 2000.
- [5] M. Franceschetti, O. Dousse, D. N. C. Tse, and P. Thiran, "Closing the gap in the capacity of wireless networks via percolation theory," *IEEE Trans. Inf. Theory*, vol. 53, no. 3, pp. 1009–1018, Mar. 2007.
- [6] P. Gupta and P. R. Kumar, "Towards an information theory of large networks: An achievable rate region," *IEEE Trans. Inf. Theory*, vol. 49, no. 8, pp. 1877–1894, Aug. 2003.
- [7] F. Xue, L.-L. Xie, and P. R. Kumar, "The transport capacity of wireless networks over fading channels," *IEEE Trans. Inf. Theory*, vol. 51, no. 3, pp. 834–847, Mar. 2005.
- [8] W.-Y. Shin, S.-Y. Chung, and Y. H. Lee, "Parallel opportunistic routing in wireless networks," *IEEE Trans. Inf. Theory*, vol. 59, no. 10, pp. 6290–6300, Oct. 2013.
- [9] A. Özgür, O. Lévéque, and D. N. C. Tse, "Hierarchical cooperation achieves optimal capacity scaling in ad hoc networks," *IEEE Trans. Inf. Theory*, vol. 53, no. 10, pp. 3549–3572, Oct. 2007.
- [10] M. Grossglauser and D. N. C. Tse, "Mobility increases the capacity of ad hoc wireless networks," *IEEE/ACM Trans. Netw.*, vol. 10, no. 4, pp. 477–486, Aug. 2002.
- [11] A. El Gamal, J. Mammen, B. Prabhakar, and D. Shah, "Optimal throughput-delay scaling in wireless networks—Part I: The fluid model," *IEEE Trans. Inf. Theory*, vol. 52, no. 6, pp. 2568–2592, Jun. 2006.
- [12] V. R. Cadambe and S. A. Jafar, "Interference alignment and degrees of freedom of the  $K$ -user interference channel," *IEEE Trans. Inf. Theory*, vol. 54, no. 8, pp. 3425–3441, Aug. 2008.
- [13] G. Zhang, Y. Xu, X. Wang, and M. Guizani, "Capacity of hybrid wireless networks with directional antennas and delay constraint," *IEEE Trans. Commun.*, vol. 58, no. 7, pp. 2097–2106, July 2010.
- [14] P. Li, C. Zhang, and Y. Fang, "The capacity of wireless ad hoc networks using directional antennas," *IEEE Trans. Mobile Comput.*, vol. 10, no. 10, pp. 1374–1387, Oct. 2011.
- [15] J. Yoon, W.-Y. Shin, and S.-W. Jeon, "Elastic routing in wireless networks with directional antennas," in *Proc. IEEE Int. Symp. Inf. Theory (ISIT)*, Honolulu, HI, Jun./Jul. 2014, pp. 1001–1005.
- [16] B. Liu, Z. Liu, and D. Towsley, "On the capacity of hybrid wireless networks," in *Proc. IEEE INFOCOM*, San Francisco, CA, Mar./Apr. 2003, pp. 1543–1552.
- [17] W.-Y. Shin, S.-W. Jeon, N. Devroye, M. H. Vu, S.-Y. Chung, Y. H. Lee, and V. Tarokh, "Improved capacity scaling in wireless networks with infrastructure," *IEEE Trans. Inf. Theory*, vol. 57, no. 8, pp. 5088–5102, Aug. 2011.
- [18] S. Gitzenis, G. S. Paschos, and L. Tassiulas, "Asymptotic laws for joint content replication and delivery in wireless networks," *IEEE Trans. Inf. Theory*, vol. 59, no. 5, pp. 2760–2776, May 2013.
- [19] M. Ji, G. Caire, and A. F. Molisch, "The throughput-outage tradeoff of wireless one-hop caching networks," *IEEE Trans. Inf. Theory*, vol. 61, no. 12, pp. 6833–6859, Dec. 2015.
- [20] S.-W. Jeon, S.-N. Hong, M. Ji, G. Caire, and A. F. Molisch, "Wireless multihop device-to-device caching networks," *IEEE Trans. Inf. Theory*, vol. 63, no. 3, pp. 1662–1676, Mar. 2017.
- [21] G. Alfano, M. Garetto, and E. Leonardi, "Content-centric wireless networks with limited buffers: When mobility hurts," *IEEE/ACM Trans. Netw.*, vol. 24, no. 1, pp. 299–311, Feb. 2016.

- [22] M. Mahdian and E. Yeh, "Throughput-delay tradeoffs in content-centric ad hoc and heterogeneous wireless networks," in *Proc. IEEE Global Telecommun. (GLOBECOM)*, San Diego, CA, Dec. 2015, pp. 1-7.
- [23] M. Mahdian and E. Yeh, "Throughput-delay tradeoffs in content-centric wireless networks," [Online]. Available: <https://arxiv.org/abs/1504.03754>.
- [24] M. A. Maddah-Ali and U. Niesen, "Fundamental limits of caching," *IEEE Trans. Inf. Theory*, vol. 60, no. 5, pp. 2856-2867, May. 2014.
- [25] M. A. Maddah-Ali and U. Niesen, "Decentralized coded caching attains order-optimal memory-rate tradeoff," *IEEE/ACM Trans. Netw.*, vol. 23, no. 4, pp. 1029-1040, Aug. 2014.
- [26] M. A. Maddah-Ali and U. Niesen, "Coding for caching: Fundamental limits and practical challenges," *IEEE Commun. Mag.*, vol. 54, no. 8, pp. 23-29, Aug. 2016.
- [27] D. E. Knuth, "Big Omicron and big Omega and big Theta," *ACM SIGACT News*, vol. 8, no. 2, pp. 18-24, Apr.-Jun. 1976.
- [28] C. Fricker, P. Robert, J. Roberts, and N. Sbihi, "Impact of traffic mix on caching performance in a content-centric network," in *Proc. IEEE INFOCOM Workshop on Emerging Choices in Named-Oriented Netw. (NoMEN)*, Orlando, FL, Mar. 2012, pp. 310-315.
- [29] S. Boyd and L. Vandenberghe, *Convex Optimization*. New York, NY, USA: Cambridge Univ. Press, 2004.
- [30] T.-A. Do, S.-W. Jeon, and W.-Y. Shin, "Caching in mobile HetNets: A throughput-delay trade-off perspective," in *Proc. IEEE Int. Symp. Inf. Theory (ISIT)*, Barcelona, Spain, Jul. 2016, pp. 1247-1251.